# ON THE VALUE OF HIGH-RESOLUTION WEATHER MODELS FOR ATMOSPHERIC MITIGATION IN SAR INTERFEROMETRY

*Shizhuo Liu, Ramon Hanssen*

Delft Institute of Earth Observation and Space Systems (DEOS)
Delft University of Technology, PO Box 5058, 2600 GB Delft
The Netherlands, {s.liu}{r.f.hanssen}@tudelft.nl

*Ágnes Mika*

BMT ARGOSS
Voorsterweg 28, 8316 PT Marknesse,
The Netherlands, agnes.mika@bmtargoss.com

## ABSTRACT

Atmospheric delay is one of the major error sources in InSAR, hindering the accurate monitoring of ground motion. Here we use the WRF (Weather Research and Forecasting) weather model to hindcast atmospheric delays at SAR acquisition times over both mountainous and flat regions. The performance of the model is evaluated by comparing it to interferograms formed using acquisitions with short temporal baselines ($\leq$4 months). Our results show that for flat regions the model not only misestimates atmospheric delay in magnitude and location but also largely underestimates the (horizontal) spatial variation (turbulent mixing) of the delay. In mountainous areas it can model the height dependent (vertical stratification) part of total delay correctly in some cases but not always. By removing the height dependent part we find again that the model may underestimate the spatial variation of the delay. Therefore, we conclude that the WRF weather model is in general not reliable for the operational mitigation of atmospheric delay in interferograms.

***Index Terms***— InSAR, numerical weather model, atmospheric delay

## 1. INTRODUCTION

Signal propagation delay induced by the troposphere affects the interferometric phase in repeat-pass SAR Interferometry (InSAR). The difficulty of modeling this delay results from the high spatiotemporal variation of water vapor. Although previous studies have proposed a number of approaches for wet delay mitigation using for instance GPS[1] or spaceborne spectrometers such as the Medium Resolution Imaging Spectrometer (MERIS)[2], these methods are only feasible under optimal conditions in terms of the spatial density of the GPS network or the absence of cloud coverage, respectively. Currently, world-wide fine-resolution (1-3 km) water vapor maps can only be obtained from Numerical Weather Models (NWM)[3]. Therefore, it is of importance to investigate the feasibility and limitations of using NWM for delay mitigation in InSAR.

Here the Weather Research and Forecasting (WRF)[4] NWM is used to estimate differential delays along the path of radar signal propagation with a spatial resolution of 1 km at the times of ENVISAT SAR acquisitions over flat areas (The Netherlands, western Australia) as well as regions with significant topography (Mexico City). The estimated differential delays are subtracted from the interferograms formed by the SAR images to mitigate the atmosphere-induced signal delay. We processed 6 interferograms over Mexico-City, 9 over the Netherlands and 5 over western Australia. All interferograms have short temporal baselines ($\leq$4 months) to suppress temporal decorrelation and to minimize possible surface deformation. Height-dependent delay (vertical stratification)[5] can be very significant in mountainous areas. We first model and then divide the total delay into a height-dependent part $D(h)$ (where $h$ is height) and a turbulent mixing component $D(x, y)$ ($x$ and $y$ are horizontal coordinates) to evaluate the performance of NWM in estimating each part separately. MERIS reduced resolution ($\sim$ 1.2 km) level 2 ($RR\_2P$) [6] water vapor products are used to verify our correction results in case the acquisitions were not severely affected by clouds.

## 2. DATA PROCESSING

### 2.1. InSAR

Differential interferograms with a pixel size of 4 by 20 meters in azimuth and range, respectively, are formed from ENVISAT ASAR acquisitions. Phase due to local surface topography is modeled and removed using 3 arc second SRTM data. After phase unwrapping the data were multilooked in a rectangular window (250 pixels in azimuth and 50 pixels in range). This increases the pixel size to 1 km in range and azimuth, which is the cell size of the NWM estimates used in our case studies. A surface trend is modeled and subtracted to remove possible trends in the data due to imperfections in orbit determination [5]. The remaining signal is considered as second-order stationary. In the end, the phase is converted to slant delay in the radar look direction.

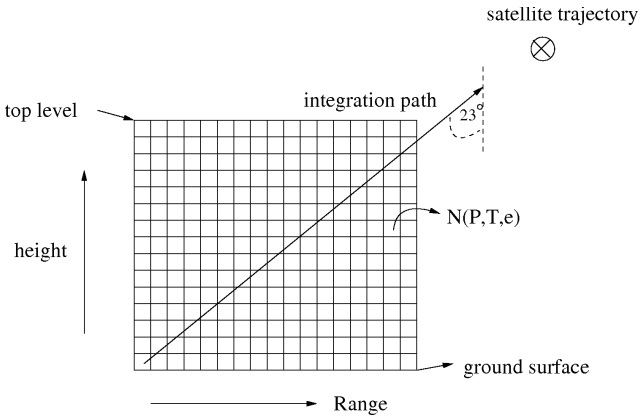


**Fig. 1**. Slant range delay integration along radar side-looking direction; the refractivity $N$ is computed for each cell; the satellite moves into the paper.

### 2.2. Numerical weather model

The WRF model was used to hindcast the meteorological conditions at the SAR acquisition times. The non-hydrostatic WRF model is a numerical weather prediction and atmospheric simulation system which can be used for both research and operational applications.

WRF is a limited-area model therefore it requires boundary conditions from a large-scale model. We use Global Final Analysis (FNL) data which are available every 6 hours. These data also serve as initial conditions for the simulations. Here we need to stress that only forward model integration is possible, meaning that FNL data from before the SAR acquisition time has to be used. We run WRF in a nested setup, with four domains of increasing horizontal resolutions of 27, 9, 3, and 1 km, respectively, to make a smooth transition from the coarse global fields to the fine target resolution.

WRF predictions 1.5 to 4.5 hours ahead, coincident with the times of the SAR acquisitions within four minutes, are used to provide the meteorological parameters needed to estimate the atmospheric delay. In our setup, the meteorological parameters, i.e. profiles of temperature ($T$ in K), total air pressure ($P$ in hPa) and partial water vapor pressure ($e$ in hPa), are estimated for every cell of the WRF grid in 3D space. The vertical profile of the estimate has 28 levels starting from the ground surface (see Fig.1). For each cell we compute the refractivity $N$ by:

$$N = k_1 \frac{P}{T} + (k_2' \frac{e}{T} + k_3 \frac{e}{T^2}), \qquad (1)$$

where $k_1 = 71.6\,\mathrm{K\,hPa^{-1}}$, $k_2' = 23.3\,\mathrm{K\,hPa^{-1}}$ and $k_3 = 3.75 \times 10^5\,\mathrm{K^2\,hPa^{-1}}$ are numerical constants [7]; the first term is the hydrostatic term induced by dry air and the second and the third terms account for the contribution from water vapor.

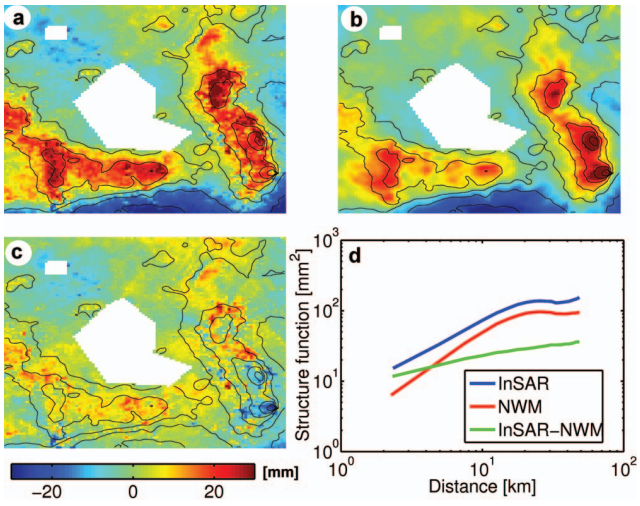


**Fig. 2**. **a**.) Original interferogram showing delay in mm; topography is presented by the black contour lines; the subsiding area is masked out; **b**.) NWM differential delay simulation; **c**.) Interferogram after correction; **d**.) Structure functions of original interferogram, NWM and corrected interferogram.

To obtain the integrated delay along the radar look direction the computed refractivities $N$ are resampled to radar coordinates (range and azimuth) followed by integration along radar side looking direction ($\theta$ =23° for ENVISAT), see Fig.1. The differential delay is computed as the difference of delay estimations during two SAR acquisitions followed by detrending to make the signal second-order stationary. In the following we will report the results of several case studies.

## 3. CASE STUDIES

### 3.1. Mexico City

Mexico City has a minimum altitude of 2200 meters above sea level and is surrounded by mountains and volcanoes that reach elevations of over 5000 meters. High subsidence rates up to 40 cm/year due to excessive ground water pumping have been observed over the urban area of the city [8]. Therefore we mask out the subsiding area in this case study.

Fig.2 presents the best result of atmospheric correction using NWM estimations. From the figure we can observe that a significant delay reduction is achieved at places where topographic gradient is large (see Fig.2c), and that the atmospheric signal in the original interferogram is effectively suppressed by NWM above wavelengths of about 5 km (see Fig.2d), though the NWM underestimates the signal variability at shorter wavelengths with respect to the original interferogram. The signal standard deviation $\sigma$ after correction is reduced from 10.8 mm to 5.4 mm.

The total delay against height (i.e. surface topography) is

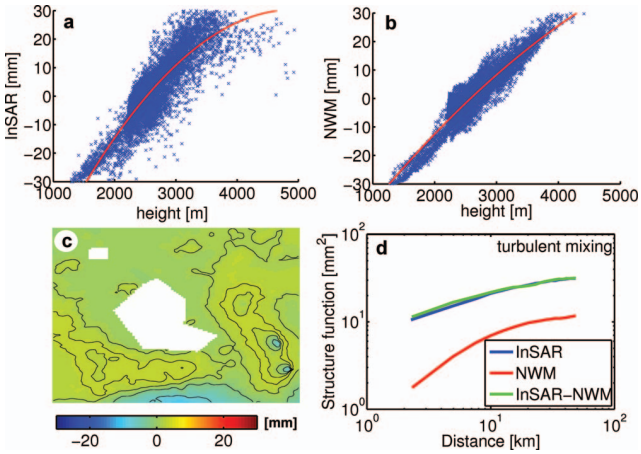


**Fig. 3**. **a**.) Original interferogram against height; **b**.) NWM against height; red curves are modeled height-dependent delay (vertical stratification) using a 2nd degree polynomial least-squares fit. **c**.) Difference of modeled vertical stratification between InSAR and NWM. Color bar in mm; **d**.) Structure functions of the residue signal (turbulent mixing) after removing the vertical stratification, interferogram (blue), NWM (red) and their difference (green).

displayed in Fig.3. It can be seen that both InSAR and NWM show very similar height-dependent delays, i.e., vertical stratification. A 2nd degree polynomial, shown as red curves in Fig.3a and b, is chosen to model the vertical stratifications using a least-squares fit. The difference between the modeled vertical stratifications (shown in Fig.3c) suggests that NWM effectively models the height-dependent part of total delay. However, the structure function of NWM shown in red in Fig.3d indicates that the horizontal variability of the delay (the turbulent mixing) is underestimated by the NWM. In addition, the structure function of the corrected interferogram shows even increased power of atmospheric signal at short wavelengths ($\leq$ 5 km) and nearly no power reduction at long wavelengths. This suggests that the physical models within WRF fail to estimate the variability of water vapor field in reality using FNL data (see Section 2.2).

Apart from the interferogram discussed above, we also corrected 5 other interferograms over the same area, as summarized in Fig.5a. Two corrected interferograms show a reduced signal standard deviation after correction, and two show show practically no improvement. Another two interferograms, however, show an increased signal standard deviation after correction. We examined one of the two interferograms using MERIS acquisitions taken simultaneously with the SAR images. The result is shown in Fig.4. The figure confirms that NWM erroneously estimates a too strong vertical stratification. Consequently, the interferometric signal is deteriorated after correction.

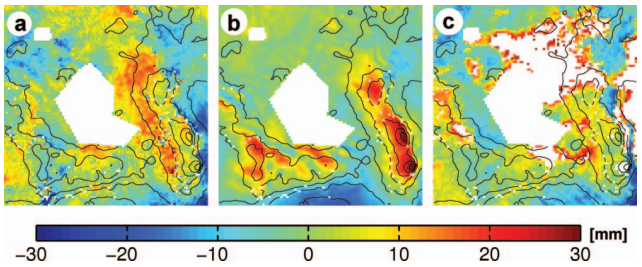


**Fig. 4**. **a**.) Differential delay observed in the interferogram; **b**.) Differential delay estimated by NWM; **c**.) Differential delay observed by MERIS (cloud pixels are masked out). Color bar is in mm.

### 3.2. Regions with flat terrain (the Netherlands, western Australia)

Scenes from the Netherlands and from western Australia are chosen in this case study. The maximum terrain height difference in these areas is less than 100 m and therefore the vertical stratification effect is negligible.

In total we corrected 5 interferograms from western Australia and 9 from the Netherlands using NWM estimations. The results are presented in Fig.5b and c. In the case of the Australian data, no reduction of delay could be achieved in any of the cases, see Fig. 5b. Over the Netherlands, see Fig. 5c, 5 out of 9 corrections show a very limited signal reduction, with a maximum of 0.3 mm for number 8. The structure functions shown in Fig.5d are for the best case in blue (interferogram 8 in Fig.5c) and the worst case in red (interferogram 4 in Fig.5c). In addition, the structure function of a single MERIS acquisition of Australia is given by the solid green line in contrast with the NWM estimation (dashed green) over that area at the same acquisition time. By comparing these structure functions it is clear to see that NWM significantly underestimates the turbulent mixing part of the delay, similar to the Mexico City case. Moreover, NWM not only underestimates the spatial variability of delay but also misestimates the delay in magnitude and location. This can be seen from the increased variation of delay after NWM correction (see Fig.5b and c). Therefore, the use of NWM estimations to correct interferograms over flat regions will not reliably lead to significant delay reduction, apart from a single opportunistic successful match. Instead, it seems likely that the correction may even deteriorate the original signal.

## 4. CONCLUSION

The results of our case studies show that in some cases NWM may effectively estimate the vertical stratification of the delay in mountainous areas. In contrary, for regions with flat terrain, NWM not only fails to correctly estimate atmospheric delay in magnitude and location but also largely underestimates the spatial variability of the delay. This is the result

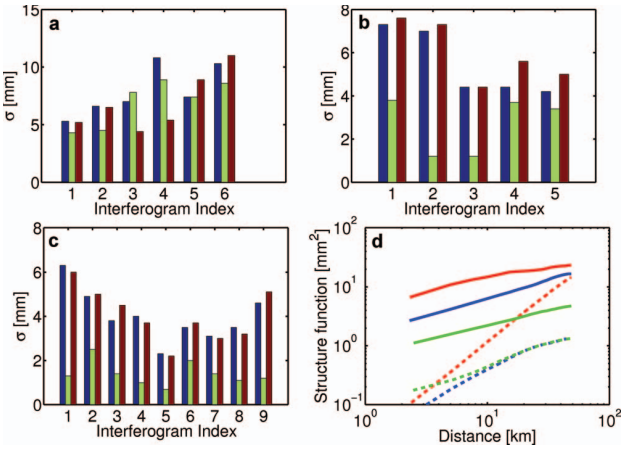


**Fig. 5**. **a**.) Results of correction using NWM for Mexico City. $x$-axis: index of the interferogram, $y$-axis: signal standard deviation [mm]. Blue, green, and red bars represent for the standard deviation of the original interferogram, NWM, and corrected interferogram, respectively. **b**.) Results for the interferograms from western Australia; **c**.) Results for the Netherlands; **d**.) Structure functions of interferogram 8 (solid blue) and 4 (solid red) of **c**.), and of the corresponding NWM simulations (dashed blue and red). In solid green the structure function of one of the Australia MERIS sets, for comparison with the corresponding NWM simulation (dashed green).

of poor estimation of the turbulent mixing (i.e. convectivity) part of the delay. Although our evaluation is based on the WRF model only, this model is expected to perform better than older generation NWMs such as e.g., NH3D and MM5 [9][3]. Therefore, we can conclude that atmospheric mitigation using NWM is currently not applicable. The reliability of its estimation largely varies from one case to the other. To be a global operationally applicable tool for correcting atmospheric induced delay in InSAR, the reliability and degree of detail of NWM estimations needs to be improved by model tuning and/or adapting more complex physical models as well as using global input data with higher spatial density.

## 5. REFERENCES


[1] S. Williams, Y. Bock, and P. Fang, "Integrated satellite interferometry: Tropospheric noise, GPS estimates and implications for interferometric synthetic aperture radar products," *Journal of Geophysical Research*, vol. 103, no. B11, pp. 27,051–27,067, 1998.

[2] Z. Li, J.-P. Muller, P. Cross, P. Albert, J. Fischer, and R. Bennartz, "Assessment of the potential of MERIS near-infrared water vapour products to correct ASAR interferometric measurements," *International Journal of Remote Sensing*, vol. 27, pp. 349–365, 2006.

[3] J. Foster, B. Brooks, T. Cherubini, C. Shacat, S. Businger, and C. L. Werner, "Mitigating atmospheric noise for InSAR using a high resolution weather model," *Geophysical Research Letters*, vol. 33, no. L16304, p. doi:10.1029/2006GL026781, 2006.

[4] "Weather Research & Forecasting (WRF) model," *http://www.wrf-model.org*, Last accessed: 4 Jan.2009.

[5] R. F. Hanssen, *Radar Interferometry: Data Interpretation and Error Analysis*. Dordrecht: Kluwer Academic Publishers, 2001.

[6] ESA, "Meris product handbook," Tech. Rep. Issue2.1, European Space Agency, 2006.

[7] J. L. Davis, T. A. Herring, I. I. Shapiro, A. E. E. Rogers, and G. Elgered, "Geodesy by radio interferometry: Effects of atmospheric modelling errors on estimates of baseline length," *Radio Science*, vol. 20, no. 6, pp. 1593–1607, 1985.

[8] T. Strozzi, U. Wegmuller, C. L. Werner, A. Wiesmann, and V. Spreckels, "JERS SAR interferometry for land subsidence monitoring," *IEEE Transactions on Geoscience and Remote Sensing*, vol. 41, pp. 1702– 1708, July 2003.

[9] G. Wadge, P. W. Webley, I. N. James, R. Bingley, A. Dodson, S. Waugh, T. Veneboer, G. Puglisi, M. Mattia, D. Baker, S. C. Edwards, S. J. Edwards, and P. J. Clarke, "Atmospheric models, gps and insar measurements of the tropospheric water vapour field over mount etna," *Geophysical Research Letters*, vol. 29, pp. 11/1–4, Oct. 2002.


### Acknowledgments


SAR and MERIS data were kindly provided by ESA. This study was funded by the ESA METAWAVE project (contract nr. 21206/07/NL/HE).